


Fibonacci wavelets operational matrix approach for solving chemistry problems

G. Manohara¹ · S. Kumbinarasaiah¹ 

Received: 20 December 2022 / Accepted: 5 April 2023

Published online: 16 May 2023

© The Author(s) 2023 

Abstract

The key idea and contribution of this study are to present the innovative functional matrix approach for solving the two chemical, mathematical problems such as the absorption of CO_2 into phenyl glycidyl ether (PGE) and the chemical kinetic problem. These chemical problems are characterized as a system of nonlinear ODEs with initial and boundary conditions. Numerical outcomes are obtained to establish the simplicity and efficacy of the developed scheme. Graphs and tables show how consistently and effectively the developed strategy works. Results obtained show that the newly adopted technique is more precise and effective than other methods such as Adam–Bashforth–Moulton method (ABM), Runge–Kutta method (RK4), Adomian Decomposition method (ADM), and residual method (RM). Mathematical software called Mathematica 11.3 has been used to perform all calculations. Theorems explain the convergence of this approach.

Keywords Chemical problems · Chemical kinetic problem · Operational matrix of integration (OMI) · Collocation technique · System of ordinary differential equations (SODEs) · Fibonacci wavelet collocation method (FWCM)

Mathematics Subject Classification 34B16 · 34A12 · 65L05 · 65L10 · 34A34

1 Introduction

In real life, many variables and parameters are connected under certain circumstances. When we mathematically represent the relationship between these variables and parameters, we usually arrive at a mathematical model of the problem: a differential equation, an integral equation, a system of differential or integral equations, etc. Mathematical modelling is the best way to formulate real-world problems. It is familiar that numerous mathematical characterizations of enormous growth in physical and chemical sciences are represented by SODEs. In the field of chemistry, the above-considered two models that are nonlinear

SODEs can describe different kinds of Dirichlet and Neumann-type boundary conditions. Carbon dioxide is vital in plant photosynthesis and the industrial of carbonated soft drinks, removing caffeine from coffee, used in fire extinguishers, and energizing pneumatic models in robotics [1, 2]. CO_2 is a beneficial gas that forms one carbon atom and two oxygen atoms. In recent times the chemical fascination of CO_2 is a significant research focus since the hazard postured by global warming and the conversion of CO_2 into valuable substances is a tremendously elegant result.

Consider the general form of the SODEs, which represents the CO_2 absorbed into the PGE problem [3]:

✉ S. Kumbinarasaiah, kumbinarasaiah@gmail.com; G. Manohara, manoharavdc15@gmail.com | ¹Department of Mathematics, Bangalore University, Bengaluru 560 056, India.



$$\left. \begin{aligned} y_1''(x) &= f_1(t, y_1(x), \dots, y_n(x), y_1'(x), \dots, y_n'(x)) \\ y_2''(x) &= f_2(t, y_1(x), \dots, y_n(x), y_1'(x), \dots, y_n'(x)) \\ &\vdots \\ y_n''(x) &= f_n(t, y_1(x), \dots, y_n(x), y_1'(x), \dots, y_n'(x)) \end{aligned} \right\} \quad (1)$$

With Dirichlet boundary conditions: $y_i(x) = \alpha_i$, $y_i(x) = \beta_i$, $i = 1, 2, \dots, n$.

Mixed set of Dirichlet and Neumann boundary conditions: $y_i'(x) = \gamma_i$, $y_i(x) = \mu_i$. Where f_1, f_2, \dots, f_n are homogeneous parts of the equation, $y_n(x)$ are the concentrations of CO_2 and PGE, respectively, α_i 's, β_i 's, γ_i 's and μ_i 's are the specified values at the different boundaries.

The mathematical model of the chemical kinetic problem is one of the well-described nonlinear SODEs that Robertson introduced in 1966. There are three spaces in the model of chemical procedure, which are indicated by P, Q, and R. We can define the three reactions as:



The concentration of P, Q, and R can be denoted by u_1, u_2 and u_3 respectively. It is worth considering that these are the combinations of three concentrations in one. Let b_1 denote the reaction rate of Eq. (2), and this means that the rate at which u_2 rises and at which u_1 reduces, due of the above reaction, it will be equivalent to $b_1 u_1$. R acts as a catalyst in the production of P from Q and b_2 represents reaction rate in the reaction Eq. (3), meaning that the decrease of u_3 and the increase of u_1 this reaction will be equivalent to $b_2 u_2 u_3$. At last, the rate at which this reaction will be equal to $b_3 u_3^2$. Due to the production of R from Q will have a constant rate equivalent to b_3 .

Consider the general form of the nonlinear SODEs, which represents the chemical kinetic problem: [4, 5]

$$u_i'(x) = g_i(x, u_1(x), u_2(x), \dots, u_q(x)) \quad (5)$$

where (') represents the derivative of the dependent variable u_i concerning the independent variable x and corresponding initial conditions; $u_i(x)_{x=0} = \alpha_i$, where α_i 's are the specified constant vector and $u_i(x)$ is the solution vector and $i = 1, 2, 3, \dots, q$. Different published works were carried out on the above models, such as the Chemistry problem by Abbasbandy and Shirzadi [6], the chemistry problem by Matinfar et al. [7], An analytical approximation to the solution of the chemical kinetic problem by Hossein A

[4], chemistry problems by Jawary and Raham [8], Kumar et al. [9] implemented a comparative study for fractional chemical kinetics and carbon dioxide CO_2 absorbed into phenyl glycidyl ether problems, CO_2 absorbed into the PGE problem by Robertson [10], Ganji et al. [5] proposed He's Homotopy Perturbation method for the chemistry kinetic problem, Jawary et al. implemented an effective iteration method and VIM (Variational Iteration Method) for the chemical kinetic problem, and the absorption of carbon dioxide into phenyl glycidyl ether problem respectively [11]. The ADM method was used for the simple steady-state condensations of CO_2 and PGE, and it is presented in [3], Duan et al. [12] successfully attempted the simple steady-state condensations of CO_2 and PGE by the ADM Method, Kaya [13] attempted the Adomian decomposition method to the chemical kinetic problem, Khader [14] applied the Laplace–Pade approximation technique to improve the performance of the Chemical Kinetic Problem (CKP) model, MSH Chowdary implemented a novel iterative method for the CK System [15], Boundary domain integral method and HAM for nonlinear BVP's were proposed by Jawary et al. [16], Singha and Wazwaz [17] proposed an optimal Homotopy analysis method for steady-state concentrations of absorption of carbon dioxide into phenyl glycidyl ether problem.

The wavelet theory is a relatively renewed and emerging theory in mathematical research. Wavelet analysis is a great tool that significantly impacts study and engineering. The primary criteria that draw researchers to the wavelet are orthogonality and effective localization. With the help of wavelets that are mathematical operations, data may be divided into several frequency components, each of which can then be analyzed at a different resolution. It is possible to employ wavelets as a mathematical tool to extract information from various data formats. Wavelet acquired the attention of many mathematics researchers for solving various types of highly nonlinear typical problems. Different wavelet collocation schemes applied for some of the common mathematical problems are Hermite, Legendre, and Laguerre wavelets [18–26], Bernoulli wavelets [28], Fractional delay differential equations [27], Fractional Riccati differential equation [29]. Few wavelet collocation methods generally used for solving various engineering, physical and biological models include Legendre wavelets [30], Haar wavelets [31–33], Chebyshev wavelets [34], Bernoulli wavelets [27, 43–45], and Ultraspherical wavelets [35, 36].

Fibonacci wavelets produced by Fibonacci polynomials are a new accumulation to the field of wavelet families. It has an added advantage in contrast with the other wavelet methods as follows [39]:

- The number of terms of the Fibonacci polynomials $P_m(x)$ is less than the number of the terms of the Legendre polynomials $L_m(x)$. It helps to reduce CPU time.
- Error components in the OMI representing Fibonacci polynomials are less than that of Legendre polynomials.
- Fibonacci polynomials $P_m(x)$ have less coefficient of individual terms than in Legendre polynomials $L_m(x)$. Computational errors can be reduced using this property.
- Using the Mathematica command `Fibonacci [m, x]`, the coefficients of the Fibonacci polynomials can be easily obtained in computer programs.

Due to its superior properties and advantages over other wavelets, it grabs the attention of many researchers. As a consequence, researchers start using this package to solve mathematical problems such as the Nonlinear Hunter–Saxton Equation [48], fractional order optimal control problems [37], time-varying delay problems [36], nonlinear Stratonovich Volterra integral equations [38], time-fractional telegraph equations [39], time-fractional bioheat transfer model [40], nonlinear Volterra integral equations [41], Dual-phase lag heat transfer model [42]. Also, some articles referred to the improvisation of concept [49–51].

This paper is organized as follows. Section 2, named “Preliminaries,” defines Fibonacci wavelets. OMI of Fibonacci wavelets carried out in Sect. 3. The method of solution and application of the proposed scheme is explained in Sects. 4 and 5, respectively. Finally, Sect. 6 gives the conclusion of the article.

2 Preliminaries of the Fibonacci wavelets

On the interval $[0, 1]$, Fibonacci wavelets are defined as [36, 39],

$$\varphi_{n,m}(x) = \begin{cases} \frac{2^{\frac{k-1}{2}}}{\sqrt{S_m}} P_m(2^{k-1}x - \hat{n}), & \frac{\hat{n}}{2^{k-1}} \leq x < \frac{\hat{n}+1}{2^{k-1}} \\ 0, & \text{Otherwise,} \end{cases}$$

with

$$S_m = \int_0^1 (P_m(x))^2 dx,$$

where $P_m(x)$ is the Fibonacci polynomial of degree $m = 0, 1, 2, \dots, M - 1$, translation parameter $n = 1, 2, \dots, 2^{k-1}$ and k represents the level of resolution $k = 1, 2, \dots$, respectively. The quantity $\frac{1}{\sqrt{S_m}}$ is a normalization factor. The Fibonacci polynomials are defined as follows in the form of the recurrence relation for every $x \in R^+$:

$$P_{m+2}(x) = xP_{m+1}(x) + P_m(x), \quad \forall m \geq 0,$$

with initial conditions $P_0(x) = 1, P_1(x) = x$.

Fibonacci wavelets are compactly supported wavelets formed by Fibonacci polynomials over the interval $[0, 1]$.

Basic Definitions [46, 47]:

Convergence: A real sequence $\{a_n\}$ converges to a limit a if for given $\epsilon > 0$, there exists $N \in \mathbb{N}$ such that if $n > N$ then $|a_n - a| < \epsilon$.

Uniform Convergence: Let E be a nonempty subset of \mathbb{R} . A sequence of functions $f_n : E \rightarrow \mathbb{R}$ is said to converge uniformly on E to a function f if and only if for every $\epsilon > 0$ there is an $N \in \mathbb{N}$ such that

$$n \geq N \text{ implies } |f_n(x) - f(x)| < \epsilon \quad \forall x \in E.$$

Absolute Continuity: A real-valued function f defined on $[a, b]$ is said to be absolutely continuous on $[a, b]$ if, given $\epsilon > 0$, there is a $\delta > 0$ such that

$$\sum_{i=1}^n |f(x'_i) - f(x_i)| < \epsilon \quad \text{whenever} \quad \sum_{i=1}^n (x'_i - x_i) < \delta.$$

Outer Measure: Let A be any set of real numbers, then the outer measure of A written as m^*A is defined by $m^*A = \inf_{A \subseteq \cup I_n} \sum_{n=1}^{\infty} l(I_n)$, where infimum is taken over the countable covering of A by open intervals.

Theorem 1 [27] Let $L^2[0, 1]$ be the Hilbert space generated by the Fibonacci wavelet basis. Let $\eta(x)$ be the continuous bounded function in $L^2[0, 1]$. Then the Fibonacci wavelet expansion of $\eta(x)$ converges with it.

Proof Let $\eta : [0, 1] \rightarrow R$ be a continuous function and $|\eta(x)| \leq \mu$, where μ be any real number. Then Fibonacci wavelet dilation of $y(x)$ can be expressed as,

$$\eta(x) = \sum_{n=1}^{2^{\frac{k-1}{2}}} \sum_{m=0}^{M-1} a_{n,m} \varphi_{n,m}(x).$$

$a_{n,m} = \langle \eta(x), \varphi_{n,m}(x) \rangle$ denotes inner product:

$$a_{n,m} = \int_0^1 \eta(x) \varphi_{n,m}(x) dx.$$

Since $\varphi_{n,m}$ are the orthogonal basis:

$$a_{n,m} = \int_l \eta(x) F_m(2^{k-1}x - n + 1) dx \quad \text{where } l = \left[\frac{n-1}{2^{k-1}}, \frac{n}{2^{k-1}} \right).$$

Then substitute $2^{k-1}x - n + 1 = y$ then we get,

$$a_{n,m} = 2^{\frac{k-1}{2}} \int_0^1 \eta \left(\frac{y+n-1}{2^{k-1}} \right) F_m(y) \frac{dy}{2^{k-1}}$$

$$a_{n,m} = 2^{\frac{1-k}{2}} \int_0^1 \eta\left(\frac{y+n-1}{2^{k-1}}\right) \sqrt{\int_0^1 S_m^2\left(\frac{y+n-1}{2^{k-1}}\right) \frac{dy}{2^{k-1}} \beta_m(y) dy}.$$

By generalized mean value theorem,

$$a_{n,m} = \frac{2^{\frac{-k+1}{2}}}{\sqrt{\frac{(-1)^{m-1}(m!)^2 \alpha_{2m}}{(2m)!}}} \eta\left(\frac{\xi+n-1}{2^{k-1}}\right) \int_0^1 \beta_m(y) dy \quad \text{for some } \xi \in (0, 1).$$

Since $\beta_m(y)$ is a bounded continuous function. Put $\int_0^1 \beta_m(y) dy = h$

$$|a_{n,m}| = \left| \frac{2^{\frac{-k+1}{2}}}{\sqrt{\frac{(-1)^{m-1}(m!)^2 \alpha_{2m}}{(2m)!}}} \eta\left(\frac{\xi+n-1}{2^{k-1}}\right) \right| h.$$

Since η remains bounded.

$$\text{Hence, } |a_{n,m}| = \left| \frac{2^{\frac{-k+1}{2}} \mu h}{\sqrt{\frac{(-1)^{m-1}(m!)^2 \alpha_{2m}}{(2m)!}}} \right|.$$

Therefore, $\sum_{n,m=0}^{\infty} a_{n,m}$ is absolutely convergent. Hence the Fibonacci wavelet series expansion $\eta(x)$ converges uniformly to it.

Theorem 2 [27] Let $I \subset R$ be a finite interval with length $m(I)$. Furthermore, $f(x)$ is an integrable function defined on I and $\sum_{i=0}^{M-1} \sum_{j=1}^{2^{k-1}} a_{ij} \varphi_{ij}(x)$ be a good Fibonacci wavelet approximation of f on I with for some $\epsilon > 0$, $|f(x) - \sum_{i=0}^{M-1} \sum_{j=1}^{2^{k-1}} a_{ij} \varphi_{ij}(x)| \leq \epsilon, \forall x \in I$. Then $-\epsilon m(I) + \int_I \sum \sum a_{ij} \varphi_{ij}(x) dx \leq \int_I f(x) dx \leq \epsilon m(I) + \int_I \sum \sum a_{ij} \varphi_{ij}(x) dx$.

3 Operational matrix of integration (OMI)

At $k=1$ and $M=10$, the Fibonacci wavelet basis is examined as follows:

$$\varphi_{1,0}(x) = 1,$$

$$\varphi_{1,1}(x) = \sqrt{3}x,$$

$$\varphi_{1,2}(x) = \frac{1}{2} \sqrt{\frac{15}{7}} (1 + x^2),$$

$$\varphi_{1,3}(x) = \sqrt{\frac{105}{239}} x(2 + x^2),$$

$$\varphi_{1,4}(x) = 3 \sqrt{\frac{35}{1943}} (1 + 3x^2 + x^4),$$

$$\varphi_{1,5}(x) = \frac{3}{4} \sqrt{\frac{385}{2582}} x(3 + 4x^2 + x^4),$$

$$\varphi_{1,6}(x) = 3 \sqrt{\frac{5005}{1268209}} (1 + 6x^2 + 5x^4 + x^6),$$

$$\varphi_{1,7}(x) = 3 \sqrt{\frac{5005}{2827883}} x(4 + 10x^2 + 6x^4 + x^6),$$

$$\varphi_{1,8}(x) = \frac{3}{2} \sqrt{\frac{85085}{28195421}} (1 + 10x^2 + 15x^4 + 7x^6 + x^8),$$

$$\varphi_{1,9}(x) = 3 \sqrt{\frac{1616615}{5016284989}} x(5 + 20x^2 + 21x^4 + 8x^6 + x^8),$$

$$\varphi_{1,10}(x) = 3 \sqrt{\frac{1616615}{11941544471}} (1 + 15x^2 + 35x^4 + 28x^6 + 9x^8 + x^{10}),$$

$$\varphi_{1,11}(x) = \frac{3}{8} \sqrt{\frac{37182145}{10276002038}} x (6 + 35x^2 + 56x^4 + 36x^6 + 10x^8 + x^{10}),$$

where,

$$\varphi_{10}(x) = [\varphi_{1,0}(x), \varphi_{1,1}(x), \varphi_{1,2}(x), \varphi_{1,3}(x), \varphi_{1,4}(x), \varphi_{1,5}(x), \varphi_{1,6}(x), \varphi_{1,7}(x), \varphi_{1,8}(x), \varphi_{1,9}(x)]^T.$$

Integrating the first ten bases described above for the range of x limits from 0 to x in the form of a linear combination of Fibonacci wavelet basis. We obtain,

$$\int_0^x \varphi_{1,0}(x) dx = \begin{bmatrix} 0 & \frac{1}{\sqrt{3}} & 0 & 0 & 0 & 0 & 0 & 0 & 0 & 0 \end{bmatrix} \varphi_{10}(x),$$

$$\int_0^x \varphi_{1,1}(x) dx = \begin{bmatrix} -\frac{\sqrt{3}}{2} & 0 & \sqrt{\frac{7}{5}} & 0 & 0 & 0 & 0 & 0 & 0 & 0 \end{bmatrix} \varphi_{10}(x),$$

$$\int_0^x \varphi_{1,2}(x) dx = \begin{bmatrix} 0 & \frac{\sqrt{5}}{6\sqrt{7}} & 0 & \frac{\sqrt{239}}{42} & 0 & 0 & 0 & 0 & 0 & 0 \end{bmatrix} \varphi_{10}(x),$$

$$\int_0^x \varphi_{1,3}(x)dx = \left[-\frac{\sqrt{105}}{2\sqrt{239}} \ 0 \ \frac{7}{2\sqrt{239}} \ 0 \ \frac{\sqrt{1943}}{4\sqrt{717}} \ 0 \ 0 \ 0 \ 0 \ 0 \right] \varphi_{10}(x),$$

$$\int_0^x \varphi_{1,4}(x)dx = \left[0 \ 0 \ 0 \ \frac{\sqrt{717}}{5\sqrt{1943}} \ 0 \ \frac{4\sqrt{2582}}{5\sqrt{21373}} \ 0 \ 0 \ 0 \ 0 \ 0 \right] \varphi_{10}(x),$$

$$\int_0^x \varphi_{1,5}(x)dx = \left[-\frac{\sqrt{385}}{4\sqrt{2582}} \ 0 \ 0 \ 0 \ \frac{\sqrt{21373}}{24\sqrt{2582}} \ 0 \ \frac{\sqrt{1268209}}{24\sqrt{33566}} \ 0 \ 0 \ 0 \ 0 \right] \varphi_{10}(x),$$

$$\overline{\varphi_{10}(x)} = \begin{bmatrix} 0 \\ 0 \\ 0 \\ 0 \\ 0 \\ 0 \\ 0 \\ 0 \\ 0 \\ \frac{\sqrt{11941544471}}{10\sqrt{5016284989}} \varphi_{1,10}(x) \end{bmatrix}.$$

Again, integrating the above ten basis, we obtain,

$$\int_0^x \varphi_{1,6}(x)dx = \left[0 \ 0 \ 0 \ 0 \ 0 \ \frac{4\sqrt{33566}}{7\sqrt{1268209}} \ 0 \ \frac{\sqrt{2827883}}{7\sqrt{1268209}} \ 0 \ 0 \right] \varphi_{10}(x),$$

$$\int_0^x \varphi_{1,7}(x)dx = \left[-\frac{3\sqrt{5005}}{4\sqrt{2827883}} \ 0 \ 0 \ 0 \ 0 \ 0 \ \frac{\sqrt{1268209}}{8\sqrt{2827883}} \ 0 \ \frac{\sqrt{28195421}}{4\sqrt{48074011}} \ 0 \right] \varphi_{10}(x),$$

$$\int_0^x \varphi_{1,8}(x)dx = \left[0 \ 0 \ 0 \ 0 \ 0 \ 0 \ 0 \ \frac{\sqrt{48074011}}{18\sqrt{28195421}} \ 0 \ \frac{\sqrt{5016284989}}{18\sqrt{535712999}} \right] \varphi_{10}(x),$$

$$\int_0^x \int_0^x \varphi_{1,0}(x)dx dx = \left[-\frac{1}{2} \ 0 \ \sqrt{\frac{7}{15}} \ 0 \ 0 \ 0 \ 0 \ 0 \ 0 \ 0 \ 0 \right] \varphi_{10}(x),$$

$$\int_0^x \varphi_{1,9}(x)dx = \left[-3\sqrt{\frac{323323}{25081424945}} \ 0 \ 0 \ 0 \ 0 \ 0 \ 0 \ 0 \ \frac{\sqrt{535712999}}{5\sqrt{5016284989}} \ 0 \right] \varphi_{10}(x) + \frac{\sqrt{11941544471}}{10\sqrt{5016284989}} \varphi_{1,10}(x).$$

Hence,

$$\int_0^x \varphi(x)dx = \mathbb{B}_{10 \times 10} \varphi_{10}(x) + \overline{\varphi_{10}(x)} \tag{6}$$

$$\int_0^x \int_0^x \varphi_{1,1}(x)dx dx = \left[0 \ -\frac{1}{3} \ 0 \ \frac{\sqrt{239}}{6\sqrt{35}} \ 0 \ 0 \ 0 \ 0 \ 0 \ 0 \right] \varphi_{10}(x),$$

where,

$$\mathbb{B}_{10 \times 10} = \begin{bmatrix} 0 & \frac{1}{\sqrt{3}} & 0 & 0 & 0 & 0 & 0 & 0 & 0 & 0 \\ -\frac{\sqrt{3}}{2} & 0 & \sqrt{\frac{7}{5}} & 0 & 0 & 0 & 0 & 0 & 0 & 0 \\ 0 & \frac{\sqrt{5}}{6\sqrt{7}} & 0 & \frac{\sqrt{239}}{42} & 0 & 0 & 0 & 0 & 0 & 0 \\ -\frac{\sqrt{105}}{2\sqrt{239}} & 0 & \frac{7}{2\sqrt{239}} & 0 & \frac{\sqrt{1943}}{4\sqrt{717}} & 0 & 0 & 0 & 0 & 0 \\ 0 & 0 & 0 & \frac{\sqrt{717}}{5\sqrt{1943}} & 0 & \frac{4\sqrt{2582}}{5\sqrt{21373}} & 0 & 0 & 0 & 0 \\ -\frac{\sqrt{385}}{4\sqrt{2582}} & 0 & 0 & 0 & \frac{\sqrt{21373}}{24\sqrt{2582}} & 0 & \frac{\sqrt{1268209}}{24\sqrt{33566}} & 0 & 0 & 0 \\ 0 & 0 & 0 & 0 & 0 & 0 & 0 & \frac{\sqrt{2827883}}{7\sqrt{1268209}} & 0 & 0 \\ -\frac{3\sqrt{5005}}{4\sqrt{2827883}} & 0 & 0 & 0 & 0 & 0 & \frac{\sqrt{1268209}}{8\sqrt{2827883}} & 0 & \frac{\sqrt{28195421}}{4\sqrt{48074011}} & 0 \\ 0 & 0 & 0 & 0 & 0 & 0 & 0 & \frac{\sqrt{48074011}}{18\sqrt{28195421}} & 0 & \frac{\sqrt{5016284989}}{18\sqrt{535712999}} \\ -3\sqrt{\frac{323323}{25081424945}} & 0 & 0 & 0 & 0 & 0 & 0 & 0 & \frac{\sqrt{535712999}}{5\sqrt{5016284989}} & 0 \end{bmatrix},$$

$$\int_0^x \int_0^x \varphi_{1,2}(x) dx dx = \left[-\frac{\sqrt{5}}{2\sqrt{21}} \ 0 \ \frac{1}{4} \ 0 \ \frac{\sqrt{1943}}{168\sqrt{3}} \ 0 \ 0 \ 0 \ 0 \ 0 \right] \varphi_{10}(x),$$

Hence,

$$\int_0^x \int_0^x \varphi(x) dx dx = \mathbf{B}' \varphi_{10}(x) + \overline{\varphi}'_{10}(x) \tag{7}$$

$$\int_0^x \int_0^x \varphi_{1,3}(x) dx dx = \left[0 \ -\frac{5\sqrt{35}}{12\sqrt{239}} \ 0 \ \frac{2}{15} \ 0 \ \frac{\sqrt{2582}}{5\sqrt{7887}} \ 0 \ 0 \ 0 \ 0 \right] \varphi_{10}(x),$$

where

$$\int_0^x \int_0^x \varphi_{1,4}(x) dx dx = \left[-\frac{\sqrt{35}}{2\sqrt{1943}} \ 0 \ \frac{7\sqrt{3}}{10\sqrt{1943}} \ 0 \ \frac{1}{12} \ 0 \ \frac{\sqrt{1268209}}{30\sqrt{277849}} \ 0 \ 0 \ 0 \right] \varphi_{10}(x),$$

$$\int_0^x \int_0^x \varphi_{1,5}(x) dx dx = \left[0 \ -\frac{\sqrt{385}}{4\sqrt{7746}} \ 0 \ \frac{\sqrt{2629}}{40\sqrt{7746}} \ 0 \ \frac{2}{35} \ 0 \ \frac{\sqrt{2827883}}{168\sqrt{33566}} \ 0 \ 0 \right] \varphi_{10}(x),$$

$$\int_0^x \int_0^x \varphi_{1,6}(x) dx dx = \left[-\frac{\sqrt{5005}}{4\sqrt{1268209}} \ 0 \ 0 \ 0 \ \frac{\sqrt{277849}}{42\sqrt{1268209}} \ 0 \ \frac{1}{24} \ 0 \ \frac{\sqrt{28195421}}{28\sqrt{21559553}} \ 0 \right] \varphi_{10}(x),$$

$$\int_0^x \int_0^x \varphi_{1,7}(x) dx dx = \left[0 \ -\frac{\sqrt{15015}}{4\sqrt{2827883}} \ 0 \ 0 \ 0 \ \frac{\sqrt{16783}}{7\sqrt{5655766}} \ 0 \ \frac{2}{63} \ 0 \ \frac{\sqrt{5016284989}}{72\sqrt{913406209}} \right] \varphi_{10}(x),$$

$$\int_0^x \int_0^x \varphi_{1,8}(x) dx dx = \left[-\frac{3\sqrt{17017}}{8\sqrt{140977105}} \ 0 \ 0 \ 0 \ 0 \ 0 \ \frac{\sqrt{21559553}}{144\sqrt{28195421}} \ 0 \ \frac{1}{40} \ 0 \right] \varphi_{10}(x) + \frac{\sqrt{11941544471}}{180\sqrt{535712999}} \varphi_{1,10}(x),$$

$$\int_0^x \int_0^x \varphi_{1,9}(x) dx dx = \left[0 \ -\sqrt{\frac{969969}{25081424945}} \ 0 \ 0 \ 0 \ 0 \ 0 \ \frac{\sqrt{913406209}}{90\sqrt{5016284989}} \ 0 \ \frac{2}{99} \right] \varphi_{10}(x) + \frac{4\sqrt{10276002038}}{55\sqrt{115374554747}} \varphi_{1,11}(x).$$

$$\mathbf{B}'_{10 \times 10} = \begin{bmatrix} -\frac{1}{2} & 0 & \sqrt{\frac{7}{15}} & 0 & 0 & 0 & 0 & 0 & 0 & 0 \\ 0 & -\frac{1}{3} & 0 & \frac{\sqrt{239}}{6\sqrt{35}} & 0 & 0 & 0 & 0 & 0 & 0 \\ -\frac{\sqrt{5}}{2\sqrt{21}} & 0 & \frac{1}{4} & 0 & \frac{\sqrt{1943}}{168\sqrt{3}} & 0 & 0 & 0 & 0 & 0 \\ 0 & -\frac{5\sqrt{35}}{12\sqrt{239}} & 0 & \frac{2}{15} & 0 & \frac{\sqrt{2582}}{5\sqrt{7887}} & 0 & 0 & 0 & 0 \\ -\frac{\sqrt{35}}{2\sqrt{1943}} & 0 & \frac{7\sqrt{3}}{10\sqrt{1943}} & 0 & \frac{1}{12} & 0 & \frac{\sqrt{1268209}}{30\sqrt{277849}} & 0 & 0 & 0 \\ 0 & -\frac{\sqrt{385}}{4\sqrt{7746}} & 0 & \frac{\sqrt{2629}}{40\sqrt{7746}} & 0 & \frac{2}{35} & 0 & \frac{\sqrt{2827883}}{168\sqrt{33566}} & 0 & 0 \\ -\frac{\sqrt{5005}}{4\sqrt{1268209}} & 0 & 0 & 0 & \frac{\sqrt{277849}}{42\sqrt{1268209}} & 0 & \frac{1}{24} & 0 & \frac{\sqrt{28195421}}{28\sqrt{21559553}} & 0 \\ 0 & -\frac{\sqrt{15015}}{4\sqrt{2827883}} & 0 & 0 & 0 & \frac{\sqrt{16783}}{7\sqrt{5655766}} & 0 & \frac{2}{63} & 0 & \frac{\sqrt{5016284989}}{72\sqrt{913406209}} \\ -\frac{3\sqrt{17017}}{8\sqrt{140977105}} & 0 & 0 & 0 & 0 & 0 & \frac{\sqrt{21559553}}{144\sqrt{28195421}} & 0 & \frac{1}{40} & 0 \\ 0 & -\sqrt{\frac{969969}{25081424945}} & 0 & 0 & 0 & 0 & 0 & \frac{\sqrt{913406209}}{90\sqrt{5016284989}} & 0 & \frac{2}{99} \end{bmatrix}$$

$$\bar{\varphi}'_{10}(x) = \begin{bmatrix} 0 \\ 0 \\ 0 \\ 0 \\ 0 \\ 0 \\ 0 \\ 0 \\ \frac{\sqrt{11941544471}}{180\sqrt{535712999}}\varphi_{1,10}(x) \\ \frac{4\sqrt{10276002038}}{55\sqrt{115374554747}}\varphi_{1,11}(x) \end{bmatrix}.$$

In the same way, we can generate matrices of different sizes for our handiness.

4 Fibonacci wavelet method

Consider the two non-linear reactions in normalized form

$$\left. \begin{aligned} y''(x) &= \frac{\eta_1 y(x)z(x)}{1+\xi_1 y(x)+\xi_2 z(x)} \\ z''(x) &= \frac{\eta_2 y(x)z(x)}{1+\xi_1 y(x)+\xi_2 z(x)} \end{aligned} \right\} \quad (8)$$

and boundary conditions will become:

$$y(0) = \alpha, y(1) = \beta, z'(0) = \gamma, z(1) = \mu \quad (9)$$

where $\eta_1, \eta_2, \xi_1, \xi_2$ are normalized arguments, $z(x)$ denotes the condensation of PGE and $y(x)$ denotes the condensation of CO₂. Here, we would like to bring the solution of system (8) that is extracted from the CO₂ absorbed into the PGE problem (1) in the Fibonacci wavelet space.

Assume that,

$$\frac{d^2y}{d^2x} \approx A^T \varphi(x) \quad (10)$$

$$\frac{d^2z}{d^2x} \approx B^T \varphi(x) \quad (11)$$

where, $A^T = [a_{1,0}, \dots, a_{1,M-1}, a_{2,0}, \dots, a_{2,M-1}, a_{2^{k-1},0}, \dots, a_{2^{k-1},M-1}]$,

$$B^T = [b_{1,0}, \dots, b_{1,M-1}, b_{2,0}, \dots, b_{2,M-1}, b_{2^{k-1},0}, \dots, b_{2^{k-1},M-1}]$$

$$\varphi(x) = [\varphi(x)_{1,0}, \dots, \varphi(x)_{1,M-1}, \varphi(x)_{2,0}, \dots, \varphi(x)_{2,M-1}, \varphi(x)_{2^{k-1},0}, \dots, \varphi(x)_{2^{k-1},M-1}].$$

Integrating the Eqs. (10) and (11) with respect to 'x' from '0' to 'x'. We get

$$y'(x) \approx y'(0) + \int_0^x A^T \varphi(x) dx$$

$$z'(x) \approx z'(0) + \int_0^x B^T \varphi(x) dx.$$

Approximating $z'(0) = \gamma$ by the Fibonacci wavelets as $z'(0) = C^T \varphi(x)$, we get

$$\left. \begin{aligned} y'(x) &\approx y'(0) + A^T [\mathbb{B}\varphi(x) + \bar{\varphi}(x)] \\ z'(x) &\approx C^T \varphi(x) + B^T [\mathbb{B}\varphi(x) + \bar{\varphi}(x)] \end{aligned} \right\} \quad (12)$$

Integrating Eq. (12) concerning 'x' between '0' and 'x' and approximating $y(0) = \alpha$ by the Fibonacci wavelets as $y(0) = D^T \varphi(x)$. We obtain

$$\left. \begin{aligned} y(x) &\approx D^T \varphi(x) + xy'(0) + A^T [\mathbb{B}\varphi'(x) + \bar{\varphi}'(x)] \\ z(x) &\approx z(0) + xC^T \varphi(x) + B^T [\mathbb{B}\varphi'(x) + \bar{\varphi}'(x)] \end{aligned} \right\} \quad (13)$$

We again express $y(1)$ and $z(1)$ in the Fibonacci wavelet as $y(1) = E^T \varphi(x)$ and $z(1) = F^T \varphi(x)$:

$$\left. \begin{aligned} y'(0) &\approx E^T \varphi(x) - D^T \varphi(1) - A^T [\mathbb{B}'\varphi(1) + \bar{\varphi}'(1)] \\ z(0) &\approx F^T \varphi(x) - C^T [\mathbb{B}\varphi(1) + \bar{\varphi}'(1)] \\ &- B^T [\mathbb{B}'\varphi(1) + \bar{\varphi}'(1)] \end{aligned} \right\} \quad (14)$$

Substituting Eqs. (14) into (13), we obtain

$$\left. \begin{aligned} y(x) &\approx D^T \varphi(x) + x(E^T \varphi(x) - D^T \varphi(1) - A^T [\mathbb{B}'\varphi(1) + \bar{\varphi}'(1)]) + A^T [\mathbb{B}\varphi(x) + \bar{\varphi}(x)] \\ z(x) &\approx F^T \varphi(x) - C^T [\mathbb{B}\varphi(1) + \bar{\varphi}'(1)] - B^T [\mathbb{B}'\varphi(1) + \bar{\varphi}'(1)] + B^T [\mathbb{B}\varphi(x) + \bar{\varphi}(x)] \end{aligned} \right\} \quad (15)$$

Now collocate (8) after substituting the above equations by following grid points $x_i = \frac{2i-1}{2^k M}, i = 1, 2 \dots M$. The system with $2^k M$ algebraic equations is obtained as shown below,

$$\left. \begin{aligned} A^T \varphi(x_i) &= \frac{\eta_1 (D^T \varphi(x_i) + x_i (E^T \varphi(x_i) - D^T \varphi(1) - A^T [\mathbb{B}'\varphi(1) + \bar{\varphi}'(1)]) + A^T [\mathbb{B}\varphi(x_i) + \bar{\varphi}(x_i)]) (F^T \varphi(x_i) - C^T [\mathbb{B}\varphi(1) + \bar{\varphi}'(1)] - B^T [\mathbb{B}'\varphi(1) + \bar{\varphi}'(1)] + B^T [\mathbb{B}\varphi(x_i) + \bar{\varphi}(x_i)])}{1 + \xi_1 (D^T \varphi(x_i) + x_i (E^T \varphi(x_i) - D^T \varphi(1) - A^T [\mathbb{B}'\varphi(1) + \bar{\varphi}'(1)]) + A^T [\mathbb{B}\varphi(x_i) + \bar{\varphi}(x_i)]) + \xi_2 (F^T \varphi(x_i) - C^T [\mathbb{B}\varphi(1) + \bar{\varphi}'(1)] - B^T [\mathbb{B}'\varphi(1) + \bar{\varphi}'(1)] + B^T [\mathbb{B}\varphi(x_i) + \bar{\varphi}(x_i)])} \\ B^T \varphi(x_i) &= \frac{\eta_2 (D^T \varphi(x_i) + x_i (E^T \varphi(x_i) - D^T \varphi(1) - A^T [\mathbb{B}'\varphi(1) + \bar{\varphi}'(1)]) + A^T [\mathbb{B}\varphi(x_i) + \bar{\varphi}(x_i)]) (F^T \varphi(x_i) - C^T [\mathbb{B}\varphi(1) + \bar{\varphi}'(1)] - B^T [\mathbb{B}'\varphi(1) + \bar{\varphi}'(1)] + B^T [\mathbb{B}\varphi(x_i) + \bar{\varphi}(x_i)])}{1 + \xi_1 (D^T \varphi(x_i) + x_i (E^T \varphi(x_i) - D^T \varphi(1) - A^T [\mathbb{B}'\varphi(1) + \bar{\varphi}'(1)]) + A^T [\mathbb{B}\varphi(x_i) + \bar{\varphi}(x_i)]) + \xi_2 (F^T \varphi(x_i) - C^T [\mathbb{B}\varphi(1) + \bar{\varphi}'(1)] - B^T [\mathbb{B}'\varphi(1) + \bar{\varphi}'(1)] + B^T [\mathbb{B}\varphi(x_i) + \bar{\varphi}(x_i)])} \end{aligned} \right\}$$

Utilizing the Secant method, solve the aforementioned equations to determine the values of the unknown Fibonacci wavelet coefficients. The numerical solution of the system (8) using the Fibonacci wavelet is obtained by substituting these coefficient values into (13).

Next, we will consider the system of ODEs, which represents the Chemical kinetic problem as follows:

$$\left. \begin{aligned} u_1'(x) &= -b_1 u_1(x) + b_2 u_2(x) u_3(x) \\ u_2'(x) &= b_1 u_1(x) - b_2 u_2(x) u_3(x) - b_3 u_2(x)^2 \\ u_3'(x) &= b_3 u_2(x)^2 \end{aligned} \right\} \quad (16)$$

and the initial conditions are : $u_1(0) = \delta_1, u_2(0) = \delta_2, u_3(0) = \delta_3$. (17)

We want to bring the solution of the SODEs in the Fibonacci wavelet space that is extracted from a chemical kinetic problem (5).

Assume that,

$$u_1'(x) \approx A^T \varphi(x) \quad (18)$$

$$u_2'(x) \approx B^T \varphi(x) \quad (19)$$

$$u_3'(x) \approx C^T \varphi(x) \quad (20)$$

where, $A^T = [a_{1,0}, \dots, a_{1,M-1}, a_{2,0}, \dots, a_{2,M-1}, a_{2^{k-1},0}, \dots, a_{2^{k-1},M-1}]$,

$B^T = [b_{1,0}, \dots, b_{1,M-1}, b_{2,0}, \dots, b_{2,M-1}, b_{2^{k-1},0}, \dots, b_{2^{k-1},M-1}]$,

$$C^T = [c_{1,0}, \dots, c_{1,M-1}, c_{2,0}, \dots, c_{2,M-1}, c_{2^{k-1},0}, \dots, c_{2^{k-1},M-1}]$$

$$\varphi(x) = [\varphi(x)_{1,0}, \dots, \varphi(x)_{1,M-1}, \varphi(x)_{2,0}, \dots, \varphi(x)_{2,M-1}, \varphi(x)_{2^{k-1},0}, \dots, \varphi(x)_{2^{k-1},M-1}]$$

We obtain the following set of equations on integrating the Eqs. (18)–(20) with respect 'x' from '0' to 'x'.

$$u_1(x) \approx u_1(0) + \int_0^x A^T \varphi(x) dx$$

$$u_2(x) \approx u_2(0) + \int_0^x B^T \varphi(x) dx$$

$$u_3(x) \approx u_3(0) + \int_0^x C^T \varphi(x) dx.$$

Using Eq. (6) and physical constraints in Eq. (17) formulated in terms of $\theta(x)$. We obtain,

$$\left. \begin{aligned} u_1(x) &\approx D^T \varphi(x) + A^T [\mathbf{B} \varphi(x) + \bar{\varphi}(x)] \\ u_2(x) &\approx E^T \varphi(x) + B^T [\mathbf{B} \varphi(x) + \bar{\varphi}(x)] \\ u_3(x) &\approx F^T \varphi(x) + C^T [\mathbf{B} \varphi(x) + \bar{\varphi}(x)] \end{aligned} \right\} \quad (21)$$

where F, D, and E are the known vectors. On Substituting Eqs. (18), (19), (20), and (21) in (16), we obtain,

Table 1 FWCM solution compared with the various methods for $y(x)$

x	FWCM solution k=1, M=6	NDSolve solution	OHAM [17]	ADM [17]	AE of FWCM with NDSolve	AE of OHAM with NDSolve	AE of ADM with NDSolve
0	0.839920073	0.839920073	0.8397515	0.8396746	6.90×10^{-12}	1.68×10^{-4}	2.45×10^{-4}
0.1	0.841750755	0.841750755	0.8415794	0.8415027	6.17×10^{-12}	1.71×10^{-4}	2.48×10^{-4}
0.2	0.847134671	0.847134671	0.8469568	0.8468806	5.47×10^{-12}	1.77×10^{-4}	2.54×10^{-4}
0.3	0.855914439	0.855914439	0.8557293	0.8556549	4.76×10^{-12}	1.85×10^{-4}	2.59×10^{-4}
0.4	0.867937884	0.867937884	0.8677478	0.8676770	4.07×10^{-12}	1.90×10^{-4}	2.60×10^{-4}
0.5	0.883056615	0.883056615	0.8828670	0.8828019	3.38×10^{-12}	1.89×10^{-4}	2.54×10^{-4}
0.6	0.901124738	0.901124738	0.9009442	0.9008874	2.70×10^{-12}	1.80×10^{-4}	2.37×10^{-4}
0.7	0.921997697	0.921997697	0.9218381	0.9217922	2.02×10^{-12}	1.59×10^{-4}	2.05×10^{-4}
0.8	0.945531270	0.945531270	0.9454074	0.9453750	1.34×10^{-12}	1.23×10^{-4}	2.56×10^{-4}
0.9	0.971580704	0.971580704	0.9715097	0.9714928	6.65×10^{-12}	7.10×10^{-4}	8.79×10^{-5}
1.0	1.000000000	1.000000000	1.0000000	1.0000000	0	0	0

Table 2 FWCM solution compared with the various methods for $z(x)$

x	FWCM solution k=1, M=6	NDSolve solution	OHAM [17]	ADM [17]	AE of FWCM with NDSolve	AE of OHAM with NDSolve	AE of ADM with NDSolve
0	1.000000000	1.000000000	1.0000000	1.0000000	0	0	0
0.1	0.942911344	0.942911344	0.9428972	0.9428979	4.15×10^{-14}	1.41×10^{-5}	1.31×10^{-5}
0.2	0.887599306	0.887599306	0.8875699	0.8875704	4.97×10^{-14}	2.94×10^{-5}	2.89×10^{-5}
0.3	0.833985194	0.833985194	0.8339414	0.8339413	6.28×10^{-14}	4.37×10^{-5}	4.30×10^{-5}
0.4	0.781992920	0.781992920	0.7819371	0.7819361	6.39×10^{-14}	5.82×10^{-5}	5.68×10^{-5}
0.5	0.731548289	0.731548289	0.7314845	0.7314823	6.21×10^{-14}	6.37×10^{-5}	6.59×10^{-5}
0.6	0.682578354	0.682578354	0.6825121	0.6825087	5.42×10^{-14}	6.62×10^{-5}	6.96×10^{-5}
0.7	0.635010837	0.635010837	0.6349490	0.6349449	4.55×10^{-14}	6.18×10^{-5}	6.59×10^{-5}
0.8	0.588773627	0.588773627	0.5887240	0.5887200	3.17×10^{-14}	4.96×10^{-5}	5.36×10^{-5}
0.9	0.543794348	0.543794348	0.5437652	0.5437627	2.44×10^{-14}	2.91×10^{-5}	3.16×10^{-5}
1.0	0.500000000	0.500000000	0.4999991	0.5000000	0	9.91×10^{-7}	0

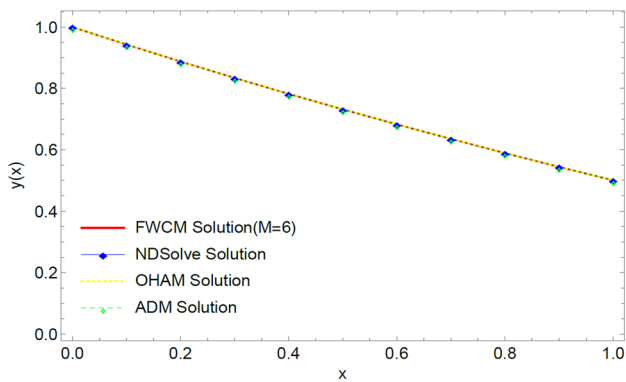


Fig. 1 The plot of FWCM solution at $k=1$ for $y(x)$ with different methods of solution

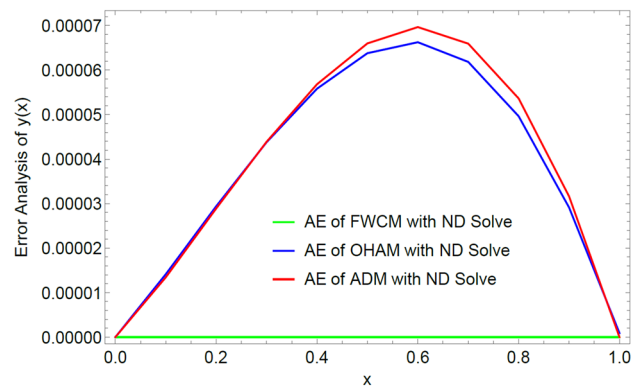


Fig. 3 Absolute error (AE) comparison of $y(x)$ at $k=1$ and $M=6$

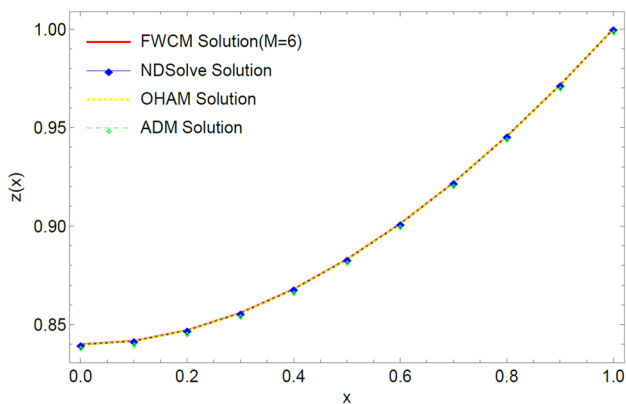


Fig. 2 A plot of FWCM solution at $k=1$ for $z(x)$ with different methods of solution

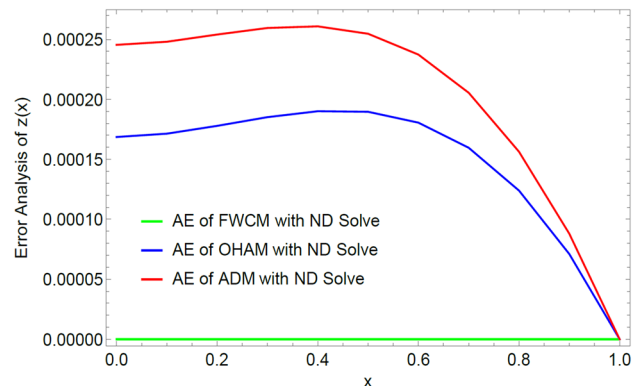


Fig. 4 Absolute error (AE) comparison of $z(x)$ at $k=1$ and $M=6$

Table 3 FWCM solution compared with the various methods for $y(x)$

x	FWCM solution $k=1, M=6$	NDSolve solution	ADM [3]	RM [42]	AE of FWCM with NDSolve	AE of ADM with NDSolve	AE of RM with NDSolve
0	1.000000000	1.000000000	1.0000	1.0000	0	0	0
0.2	0.875548854	0.875548854	0.8734	0.8730	4.97×10^{-14}	2.14×10^{-3}	2.14×10^{-3}
0.4	0.764556398	0.764556398	0.7614	0.7610	6.39×10^{-14}	3.15×10^{-3}	3.15×10^{-3}
0.6	0.665735378	0.665735378	0.6629	0.6626	5.42×10^{-14}	2.83×10^{-3}	2.83×10^{-3}
0.8	0.577912192	0.577912192	0.5762	0.5761	3.17×10^{-14}	1.71×10^{-3}	1.71×10^{-3}
1.0	0.500000000	0.500000000	0.5000	0.5000	0	5.55×10^{-17}	5.55×10^{-17}

Table 4 FWCM solution compared with the various methods for $z(x)$

x	FWCM solution $k=1, M=6$	NDSolve solution	ADM [3]	RM [42]	AE of FWCM with NDSolve	AE of ADM with NDSolve	AE of RM with NDSolve
0	0.841773796	0.841773796	0.8420	0.8426	6.90×10^{-12}	2.26×10^{-4}	8.26×10^{-4}
0.2	0.848967891	0.848967891	0.8491	0.8497	5.47×10^{-12}	1.32×10^{-4}	7.32×10^{-4}
0.4	0.869620676	0.869620676	0.8698	0.8701	4.07×10^{-12}	1.79×10^{-4}	4.79×10^{-4}
0.6	0.902444897	0.902444897	0.9021	0.9026	2.70×10^{-12}	3.44×10^{-4}	1.55×10^{-4}
0.8	0.946266951	0.946266951	0.9459	0.9462	1.34×10^{-12}	3.66×10^{-4}	0.66×10^{-4}
1.0	1.000000000	1.000000000	0.1000	0.1000	0	0	0

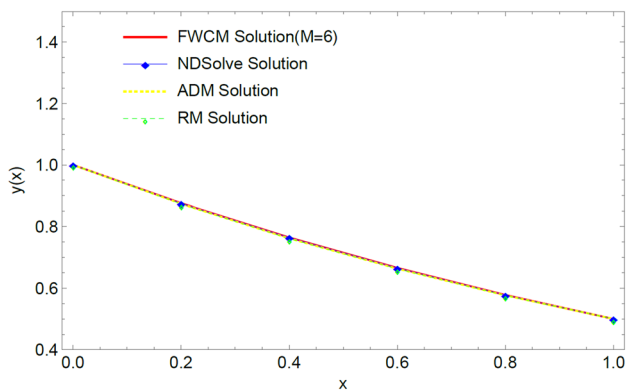


Fig. 5 The plot of FWCM solution at $k=1$ for $y(x)$ with different methods of solution

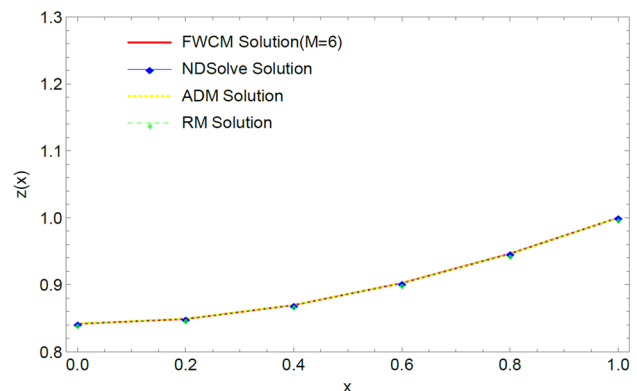


Fig. 6 The plot of FWCM solution at $k=1$ for $z(x)$ with different methods of solution

$$\left. \begin{aligned}
 A^T \varphi(x) &\approx -b_1 (D^T \varphi(x) + A^T [\mathbf{B}\varphi(x) + \bar{\varphi}(x)]) + b_2 (E^T \varphi(x) + B^T [\mathbf{B}\varphi(x) + \bar{\varphi}(x)]) \\
 (F^T \varphi(x) + C^T [\mathbf{B}\varphi(x) + \bar{\varphi}(x)]) \\
 B^T \varphi(x) &\approx b_1 (D^T \varphi(x) + A^T [\mathbf{B}\varphi(x) + \bar{\varphi}(x)]) - b_2 (E^T \varphi(x) + B^T [\mathbf{B}\varphi(x) + \bar{\varphi}(x)]) \\
 (F^T \varphi(x) + C^T [\mathbf{B}\varphi(x) + \bar{\varphi}(x)]) - b_3 (E^T \varphi(x) + B^T [\mathbf{B}\varphi(x) + \bar{\varphi}(x)])^2 \\
 C^T \varphi(x) &\approx b_3 (E^T \varphi(x) + B^T [\mathbf{B}\varphi(x) + \bar{\varphi}(x)])^2
 \end{aligned} \right\} \quad (22)$$

On collocating all the equations of (22) by using the grid points $x_i = \frac{2i-1}{2^k M}, i = 1, 2 \dots M$, we arrive the system with $2^k M$ algebraic equations as below:

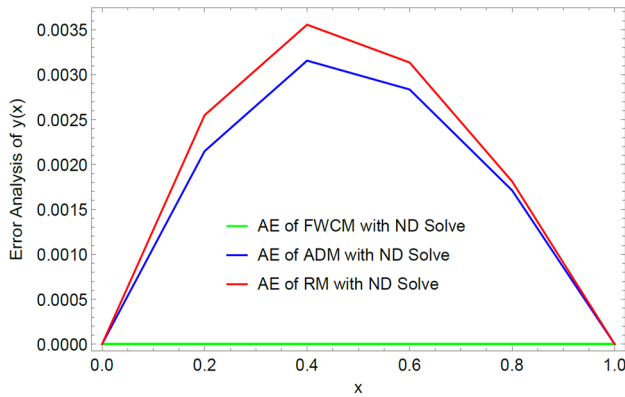


Fig. 7 Absolute error (AE) comparison of $y(x)$ at $k=1$ and $M=6$ with different methods in the literature

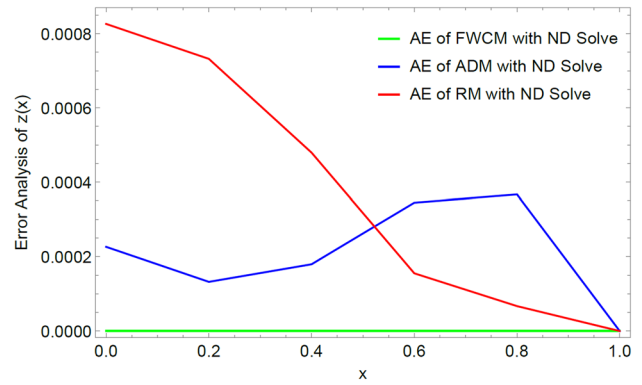


Fig. 8 Absolute error (AE) comparison of $z(x)$ at $k=1$ and $M=6$ with different methods in the literature

$$\left. \begin{aligned}
 A^T \varphi(x_i) &\approx -b_1 (D^T \varphi(x_i) + A^T [\mathbf{B}\varphi(x_i) + \bar{\varphi}(x_i)]) + b_2 (E^T \varphi(x_i) + B^T [\mathbf{B}\varphi(x_i) + \bar{\varphi}(x_i)]) \\
 (F^T \varphi(x_i) + C^T [\mathbf{B}\varphi(x_i) + \bar{\varphi}(x_i)]) \\
 B^T \varphi(x_i) &\approx b_1 (D^T \varphi(x_i) + A^T [\mathbf{B}\varphi(x_i) + \bar{\varphi}(x_i)]) - b_2 (E^T \varphi(x_i) + B^T [\mathbf{B}\varphi(x_i) + \bar{\varphi}(x_i)]) \\
 (F^T \varphi(x_i) + C^T [\mathbf{B}\varphi(x_i) + \bar{\varphi}(x_i)]) - b_3 (E^T \varphi(x_i) + B^T [\mathbf{B}\varphi(x_i) + \bar{\varphi}(x_i)])^2 \\
 C^T \varphi(x_i) &\approx b_3 (E^T \varphi(x_i) + B^T [\mathbf{B}\varphi(x_i) + \bar{\varphi}(x_i)])^2
 \end{aligned} \right\} \tag{23}$$

Utilizing the Newton–Raphson/Secant method, solve the aforementioned equations to determine the values of the unknown Fibonacci wavelet coefficients. The numerical solution of the system (16) using the Fibonacci wavelet is obtained by substituting these coefficient values into (21).

5 Numerical results and discussion

Example 5.1 The non-linear SODEs of the CO₂ absorbed into phenyl glycidyl ether problem is of the form

$$\left. \begin{aligned}
 y''(x) &= \frac{\eta_1 y(x)z(x)}{1 + \xi_1 y(x) + \xi_2 z(x)} \\
 z''(x) &= \frac{\eta_2 y(x)z(x)}{1 + \xi_1 y(x) + \xi_2 z(x)}
 \end{aligned} \right\} \tag{24}$$

Table 5 FWCM solution compared with the various approaches for $u_1(x)$

x	FWCM solution k=1, M=6	ND Solve solution	Runge–Kutta method	ABM [9]	AE of FWCM with NDSolve	AE of RK4 with NDSolve	AE of ABM with NDSolve
0	0.000000000	0.000000000	0.000000000	0.0000000	0.0000000	6.61×10^{-24}	6.61×10^{-24}
0.1	2.9775×10^{-8}	3.2018×10^{-8}	2.9776×10^{-8}	4.0×10^{-8}	1.18×10^{-14}	4.69×10^{-13}	1.02×10^{-8}
0.2	2.3643×10^{-7}	2.3617×10^{-7}	2.3643×10^{-7}	2.7×10^{-7}	1.19×10^{-14}	4.69×10^{-13}	3.35×10^{-8}
0.3	7.0292×10^{-7}	7.9135×10^{-7}	7.9202×10^{-7}	8.6×10^{-7}	1.36×10^{-14}	5.16×10^{-11}	6.79×10^{-8}
0.4	1.8634×10^{-6}	1.8625×10^{-6}	1.8635×10^{-6}	1.9×10^{-6}	1.46×10^{-14}	2.13×10^{-10}	3.66×10^{-8}
0.5	3.6126×10^{-6}	3.6115×10^{-6}	3.6129×10^{-6}	3.8×10^{-6}	1.43×10^{-14}	6.42×10^{-10}	1.87×10^{-7}
0.6	6.1964×10^{-6}	6.1954×10^{-6}	6.1971×10^{-6}	6.4×10^{-6}	1.77×10^{-14}	1.58×10^{-9}	2.04×10^{-7}
0.7	9.7671×10^{-6}	9.7661×10^{-6}	9.7686×10^{-6}	1.0×10^{-5}	2.37×10^{-14}	3.37×10^{-9}	2.34×10^{-7}
0.8	1.4472×10^{-5}	1.4471×10^{-5}	1.4475×10^{-5}	1.5×10^{-5}	2.37×10^{-14}	6.51×10^{-9}	5.31×10^{-7}
0.9	2.0454×10^{-5}	2.0453×10^{-5}	2.0459×10^{-5}	2.0×10^{-5}	2.37×10^{-14}	1.16×10^{-8}	4.48×10^{-7}
1.0	2.7857×10^{-5}	2.7851×10^{-5}	2.7861×10^{-5}	2.8×10^{-5}	2.37×10^{-14}	1.94×10^{-8}	1.58×10^{-7}

Table 6 FWCM solution compared with the various approaches for $u_2(x)$

x	FWCM solution k=1, M=6	ND Solve solution	Runge–Kutta	ABM [9]	AE of FWCM with NDSolve	AE of RK4 with NDSolve	AE of ABM with NDSolve
0	0.000000000	0.000000000	0.000000000	0.0000	0	0	0
0.1	0.009950136	0.009950182	0.009950196	0.0107	3.46×10^{-14}	5.95×10^{-8}	7.49×10^{-4}
0.2	0.019801090	0.019801350	0.019801563	0.0206	3.46×10^{-14}	4.72×10^{-7}	7.98×10^{-4}
0.3	0.029553674	0.029554544	0.029555258	0.0303	6.93×10^{-14}	1.58×10^{-6}	7.46×10^{-4}
0.4	0.039208697	0.039210743	0.039212424	0.0400	6.93×10^{-14}	3.72×10^{-6}	7.91×10^{-4}
0.5	0.048766962	0.048770923	0.048774188	0.0495	6.93×10^{-14}	7.22×10^{-6}	7.33×10^{-4}
0.6	0.058229269	0.058236048	0.058241664	0.0590	6.93×10^{-14}	1.23×10^{-5}	7.70×10^{-4}
0.7	0.067596412	0.067607072	0.067615950	0.0683	2.41×10^{-14}	1.95×10^{-5}	7.03×10^{-4}
0.8	0.076869181	0.076884937	0.076898132	0.0776	1.38×10^{-14}	2.89×10^{-5}	7.30×10^{-4}
0.9	0.086048360	0.086070573	0.086089280	0.0868	1.38×10^{-14}	4.09×10^{-5}	7.51×10^{-4}
1.0	0.095134729	0.095164901	0.095190453	0.0962	4.84×10^{-14}	5.57×10^{-5}	1.06×10^{-3}

Table 7 FWCM solution compared with the various approaches for $u_3(x)$

x	FWCM solution k=1, M=6	NDSolve solution	Runge–Kutta	ABM [9]	AE of FWCM with NDSolve	AE of RK4 with NDSolve	AE of ABM with NDSolve
0	1.000000000	1.000000000	1.000000000	1.0000	0	0	0
0.1	0.990049833	0.990049833	0.990049833	0.9893	0	6.02×10^{-13}	7.49×10^{-4}
0.2	0.980198673	0.980198673	0.980198673	0.9794	1.11×10^{-14}	5.83×10^{-12}	7.98×10^{-4}
0.3	0.970445533	0.970445533	0.970445533	0.9697	1.11×10^{-14}	5.37×10^{-11}	7.45×10^{-4}
0.4	0.960789432	0.960789439	0.960789439	0.9600	1.11×10^{-14}	2.30×10^{-10}	7.89×10^{-4}
0.5	0.951229424	0.951229424	0.951229424	0.9505	1.11×10^{-14}	7.02×10^{-10}	7.29×10^{-4}
0.6	0.941764534	0.941764534	0.941764532	0.9410	1.11×10^{-14}	1.73×10^{-9}	7.64×10^{-4}
0.7	0.932393821	0.932393821	0.932393818	0.9317	1.11×10^{-14}	3.70×10^{-9}	6.93×10^{-4}
0.8	0.923116345	0.923116349	0.923116342	0.9224	1.11×10^{-14}	7.13×10^{-9}	7.16×10^{-4}
0.9	0.913931191	0.913931191	0.913931178	0.9132	1.11×10^{-14}	1.27×10^{-8}	7.31×10^{-4}
1.0	0.904837428	0.904837428	0.904837407	0.9041	1.11×10^{-14}	2.12×10^{-8}	7.37×10^{-4}

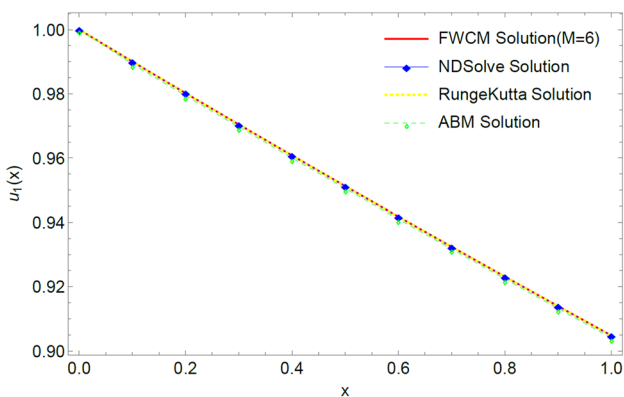


Fig. 9 The plot of the FWCM solution at k=1 for $u_1(x)$ with different methods of solution

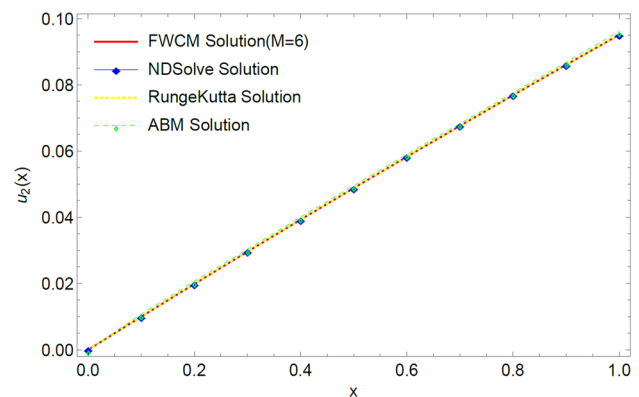


Fig. 10 The plot of the FWCM solution at k=1 for $u_2(x)$ with different methods of solution

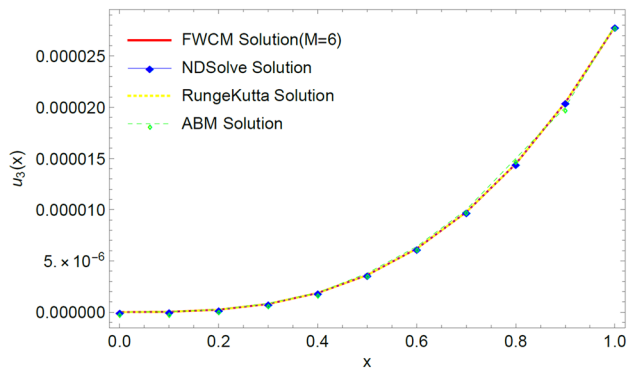


Fig. 11 The plot of the FWCM solution at $k=1$ for $u_3(x)$ with different methods of solution

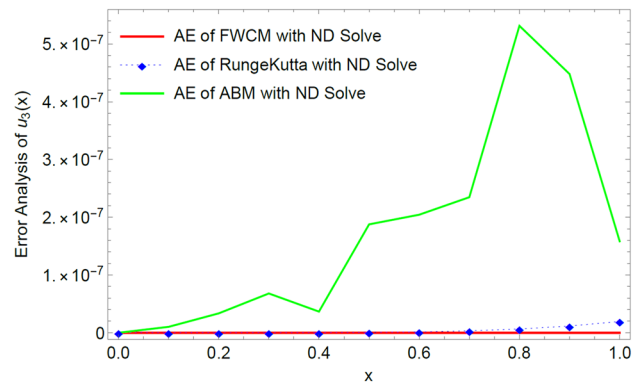


Fig. 14 Absolute error (AE) comparison of $u_3(x)$ at $k=1$ and $M=6$ with distinct approaches in the literature

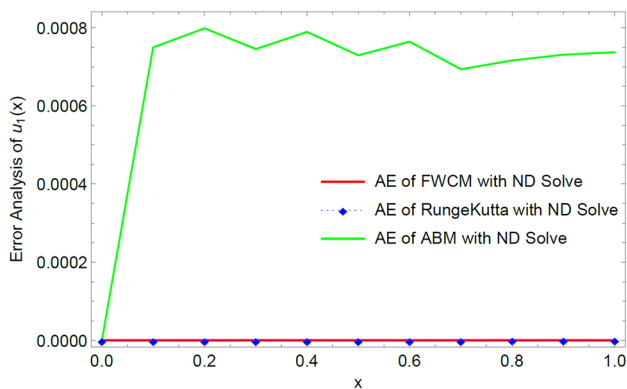


Fig. 12 Absolute error (AE) comparison of $u_1(x)$ at $k=1$ and $M=6$ with different methods in the literature

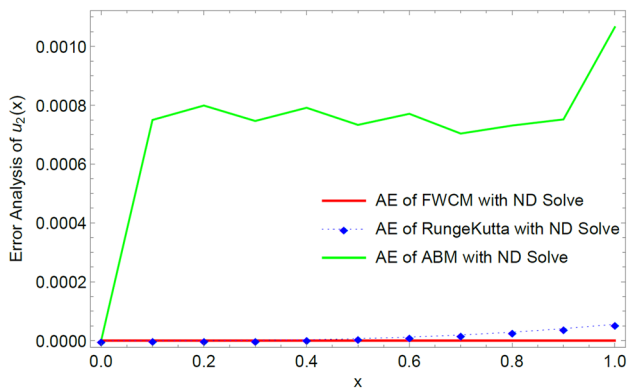


Fig. 13 Absolute error (AE) comparison of $u_2(x)$ at $k=1$ and $M=6$ with distinct approaches in the literature

and the boundary conditions will be : (25)
 $y(0) = \alpha, y(1) = \beta, z'(0) = \gamma, z(1) = \mu$

Case 1: $\eta_1 = 1, \eta_2 = 2, \xi_1 = 1, \xi_2 = 3, \alpha = 1, \beta = 0.5, \gamma = 0, \mu = 1$. Tables 1 and 2 and Figs. 1, 2, 3, and 4 depict all the

numerical simulations and graphical results of this particular case. We have compared the proposed method with the optimal homotopy analysis method (OHAM) [17], the Adomian decomposition method (ADM) [17], and the ND Solve solution due to the non-availability of the exact solution. It can be observed that the FWCM solution is very much close to the NDSolve solution. The CPU time taken is 1.017 s for the two tables of values together.

Case 2: $\eta_1 = 2, \eta_2 = 2, \xi_1 = 1, \xi_2 = 3, \alpha = 1, \beta = 0.5, \gamma = 0, \mu = 1$. Tables 3 and 4 and Figs. 5, 6, 7 and 8 depict this case's numerical simulations and graphical results. We have compared the proposed method (FWCM) with the Adomian Decomposition method (ADM), Residual method (RM), and ND solve solution due to the non-availability of the exact solution. It can be observed that the FWCM solution is very close to the NDSolve solution. The CPU time taken is 1.827 s for the two tables of values together.

Example 5.2 Next, Consider the system of ODEs of Chemical Kinetic Problem as follows:

$$u_1'(x) = -b_1 u_1(x) + b_2 u_2(x) u_3(x)$$

$$u_2'(x) = b_1 u_1(x) - b_2 u_2(x) u_3(x) - b_3 u_2(x)^2$$

$$u_3'(x) = b_3 u_2(x)^2.$$

And the physical constraints are:
 $u_1(0) = 1, u_2(0) = 0, u_3(0) = 0$.

Tables 5, 6 and 7 and Figs. 9, 10, 11, 12, 13 and 14 depict this problem's numerical simulations and graphical results. We have compared the proposed method (FWCM) solution with the Adam–Bashforth–Moulton method (ABM), Runge–Kutta method (RK4), and ND Solve solution due to the non-availability of the exact solution. It can be

Table 8 Comparison of Absolute error (AE) with different values of k and M for $u_1(x)$

x	AE of FWCM (k=1, M=4) with NDSolve	AE of FWCM (k=2, M=4) with NDSolve	AE of FWCM (k=1, M=6) with NDSolve	AE of FWCM (k=2, M=6) with NDSolve
0	0	0	0	0
0.1	4.36×10^{-10}	4.42×10^{-14}	1.20×10^{-11}	2.22×10^{-16}
0.2	3.80×10^{-10}	3.13×10^{-14}	7.20×10^{-12}	3.33×10^{-16}
0.3	2.54×10^{-10}	3.04×10^{-14}	1.08×10^{-11}	2.22×10^{-16}
0.4	2.22×10^{-10}	3.34×10^{-14}	5.98×10^{-12}	3.33×10^{-16}
0.5	2.80×10^{-10}	3.16×10^{-14}	1.20×10^{-16}	2.22×10^{-16}
0.6	3.37×10^{-10}	2.97×10^{-14}	1.20×10^{-11}	3.33×10^{-16}
0.7	3.04×10^{-10}	3.27×10^{-14}	7.16×10^{-12}	3.33×10^{-16}
0.8	1.77×10^{-10}	3.18×10^{-14}	1.08×10^{-11}	3.33×10^{-16}
0.9	1.24×10^{-10}	1.95×10^{-14}	5.95×10^{-12}	1.95×10^{-16}
1.0	5.67×10^{-10}	6.18×10^{-14}	1.80×10^{-11}	4.44×10^{-16}

Table 9 Comparison of Absolute error (AE) with different values of k and M for $u_2(x)$

x	AE of FWCM (k=1, M=4) with NDSolve	AE of FWCM (k=2, M=4) with NDSolve	AE of FWCM (k=1, M=6) with NDSolve	AE of FWCM (k=2, M=6) with NDSolve
0	0	0	0	0
0.1	1.11×10^{-10}	7.67×10^{-14}	3.56×10^{-12}	4.56×10^{-16}
0.2	1.03×10^{-10}	5.46×10^{-14}	2.33×10^{-12}	4.96×10^{-16}
0.3	7.76×10^{-10}	5.32×10^{-14}	3.43×10^{-12}	4.51×10^{-16}
0.4	7.32×10^{-11}	5.88×10^{-14}	2.28×10^{-12}	4.92×10^{-16}
0.5	8.89×10^{-11}	5.57×10^{-14}	6.98×10^{-16}	6.93×10^{-16}
0.6	1.05×10^{-10}	5.27×10^{-14}	2.35×10^{-12}	4.02×10^{-16}
0.7	1.02×10^{-10}	5.83×10^{-14}	1.59×10^{-11}	4.44×10^{-16}
0.8	7.99×10^{-11}	5.68×10^{-14}	2.32×10^{-12}	3.88×10^{-16}
0.9	7.09×10^{-11}	3.52×10^{-14}	1.64×10^{-12}	4.02×10^{-16}
1.0	1.57×10^{-10}	1.10×10^{-13}	3.61×10^{-12}	8.18×10^{-16}

Table 10 Comparison of Absolute error (AE) with different values of k and M for $u_3(x)$

x	AE of FWCM (k=1, M=4) with NDSolve	AE of FWCM (k=2, M=4) with NDSolve	AE of FWCM (k=1, M=6) with NDSolve	AE of FWCM (k=2, M=6) with NDSolve
0	6.61×10^{-24}	6.61×10^{-24}	6.61×10^{-24}	6.61×10^{-24}
0.1	5.47×10^{-10}	3.25×10^{-14}	1.56×10^{-11}	1.81×10^{-16}
0.2	4.83×10^{-10}	2.33×10^{-14}	9.53×10^{-12}	1.97×10^{-16}
0.3	3.31×10^{-10}	2.28×10^{-14}	1.43×10^{-11}	1.79×10^{-16}
0.4	2.95×10^{-11}	2.53×10^{-14}	8.27×10^{-12}	1.95×10^{-16}
0.5	3.61×10^{-11}	2.41×10^{-14}	1.35×10^{-20}	1.48×10^{-16}
0.6	4.42×10^{-10}	2.30×10^{-14}	1.43×10^{-11}	1.82×10^{-16}
0.7	4.06×10^{-10}	2.55×10^{-14}	8.57×10^{-12}	1.98×10^{-16}
0.8	2.57×10^{-11}	2.50×10^{-14}	1.31×10^{-11}	1.80×10^{-16}
0.9	1.95×10^{-11}	1.58×10^{-14}	7.59×10^{-12}	1.96×10^{-16}
1.0	7.25×10^{-10}	4.84×10^{-14}	2.17×10^{-11}	3.78×10^{-16}

Table 11 FWCM solution compared with the various approaches for $w_1(x)$

x	Exact solution	FWCM $k=1, M=6$	NDSolve solution	AE of FWCM with Exact solution	AE of NDSolve with Exact solution
0	0	0	0	0	0
0.1	-0.099	-0.099	-0.09900000	2.77×10^{-17}	2.44×10^{-15}
0.2	-0.192	-0.192	-0.19200000	8.32×10^{-17}	3.21×10^{-15}
0.3	-0.273	-0.273	-0.27300000	5.55×10^{-17}	3.99×10^{-15}
0.4	-0.336	-0.336	-0.33600000	1.11×10^{-16}	4.88×10^{-15}
0.5	-0.375	-0.375	-0.37500000	1.66×10^{-16}	6.05×10^{-15}
0.6	-0.384	-0.384	-0.38400000	2.22×10^{-16}	7.43×10^{-15}
0.7	-0.357	-0.357	-0.35700000	3.88×10^{-16}	8.88×10^{-15}
0.8	-0.288	-0.288	-0.28800000	2.22×10^{-16}	9.71×10^{-15}
0.9	-0.171	-0.171	-0.17100000	3.05×10^{-16}	8.02×10^{-15}
1.0	0	4.79×10^{-16}	-1.57×10^{-15}	4.79×10^{-16}	1.54×10^{-15}

Table 12 FWCM solution compared with the various approaches for $w_2(x)$

x	Exact solution	FWCM $k=1, M=6$	NDSolve solution	AE of FWCM with exact solution	AE of NDSolve with exact solution
0	0	0	0	0	0
0.1	0.09	0.09	0.09000000	2.77×10^{-17}	2.44×10^{-15}
0.2	-0.16	-0.16	-0.16000000	8.32×10^{-17}	3.21×10^{-15}
0.3	-0.21	-0.21	-0.21000000	5.55×10^{-17}	3.99×10^{-15}
0.4	-0.24	-0.24	-0.24000000	1.11×10^{-16}	4.88×10^{-15}
0.5	-0.25	-0.25	-0.25000000	1.66×10^{-16}	6.05×10^{-15}
0.6	-0.24	-0.24	-0.24000000	2.22×10^{-16}	7.43×10^{-15}
0.7	-0.21	-0.21	-0.21000000	3.88×10^{-16}	8.88×10^{-15}
0.8	-0.16	-0.16	-0.16000000	2.22×10^{-16}	9.71×10^{-15}
0.9	-0.09	-0.09	-0.09000000	3.05×10^{-16}	8.02×10^{-15}
1.0	0	3.7×10^{-17}	1.41×10^{-15}	4.79×10^{-16}	1.54×10^{-15}

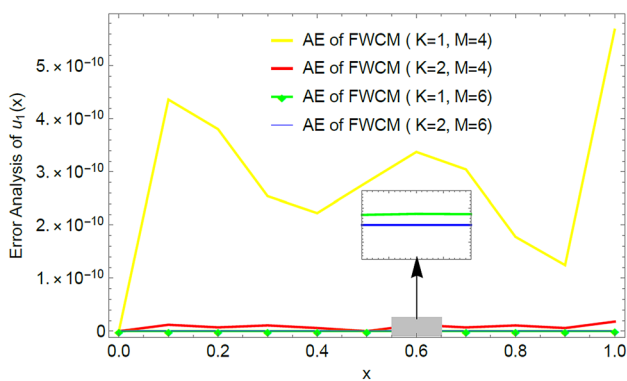


Fig. 15 AE comparison for $u_1(x)$ at various values of M and k

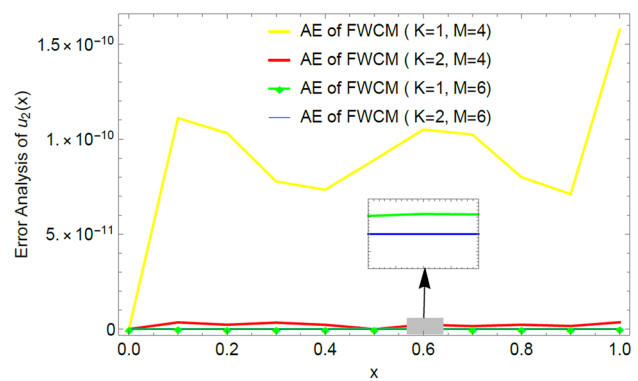


Fig. 16 AE comparison for $u_2(x)$ at various values of M and k

observed that the FWCM solution is very much close to the ND Solve solution. It is clear from the Tables and Graphs that the approximate solution obtained from the FWCM is close to the ND Solve solution, which shows the efficiency

of the proposed method. Also, we got a better solution by increasing the value of M and k , which can be seen in Tables 8, 9 and 10. Comparison of AE with distinct values

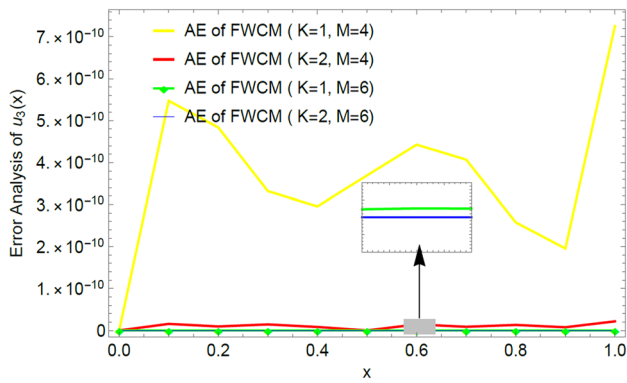


Fig. 17 AE comparison for $u_3(x)$ at various values of M and k

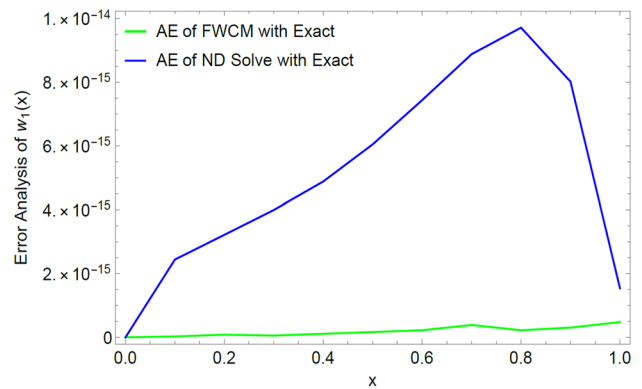


Fig. 20 Absolute error (AE) comparison of $w_1(x)$ at k=1 and M=6 with ND solve

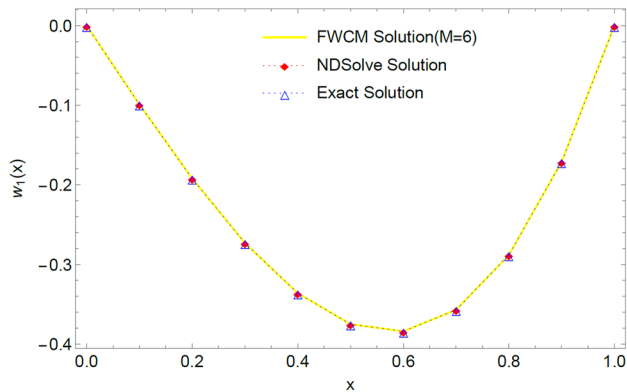


Fig. 18 The plot of the FWCM solution at k=1 for $w_1(x)$ with exact and NDSolve solutions

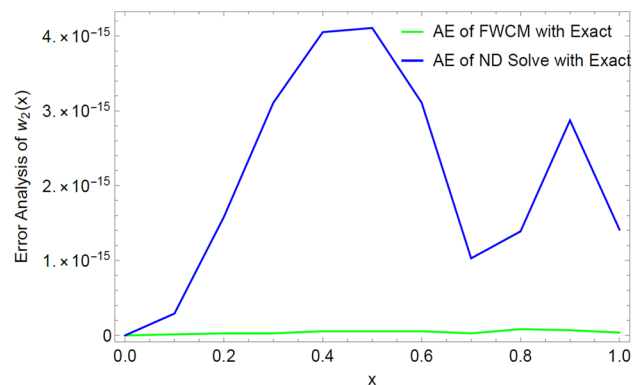


Fig. 21 Absolute error (AE) comparison of $w_2(x)$ at k=1 and M=6 with ND solve

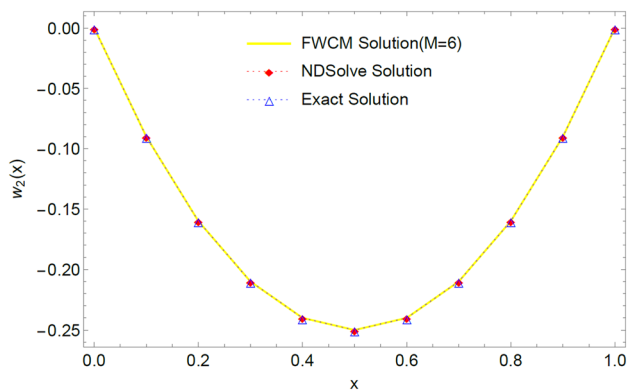


Fig. 19 The plot of the FWCM solution at k=1 for $w_2(x)$ with exact and NDSolve solutions

Example 5.3 Perhaps we will consider one more system of nonlinear ODEs in which the exact solution is available to examine the performance of the novel technique FWCM [4]:

$$w_1''(x) = xw_1'(x) - w_1 + x^3 - 2x^2 + 6x$$

$$w_2''(x) = -xw_1' - w_1w_2 + x^5 - x^4 + 2x^3 + x^2 - x + 2$$

With boundary conditions: $w_1(0) = 0, w_1(1) = 0, w_2(0) = 0, w_2(1) = 0$.

The Exact solutions of the above system are: $w_1(x) = x^3 - x, w_2(x) = x^2 - x$. We compared the solutions obtained from the FWCM and ND Solve methods with the Exact solutions in Tables 11 and 12. Also, we brought the Absolute Errors of FWCM and NDSolve method with the exact solutions in the same tables. Graphical comparison of solutions and absolute errors are exposed in Graphs 18–21. Tables and Graphs reveal the precision and

of M and k are presented in graphs 15–17. The CPU time taken is 0.891 s for all three tables of values together.

efficacy of the developed method. The CPU time taken is 0.594 s for the tables of values together.

6 Conclusion

In this article, we have implemented a new collocation approach called the Fibonacci wavelet collocation method (FWCM). The functional matrix of integration is obtained by using the Fibonacci wavelets. We solved two nonlinear SODEs representing the two familiar chemistry models using this matrix. The accuracy and proficiency of this novel technique were demonstrated by comparing the obtained solutions with other standard methods such as RK4 and ND Solve. Tables and Graphs reveal that the FWCM converges rapidly compared to other existing techniques (ADM, RM, HPM, and VIM) in the literature. Also, numerical illustrations support the claim that only a few Fibonacci wavelets are sufficient to obtain satisfactory results. Hence the proposed method is a very attractive and efficient numerical technique to solve different chemical, biological, and physical problems. From Tables 8, 9, and 10 and Figs. 15, 16, and 17, we can see that the values of k and M increases the accuracy of the solution. The future recommendation of the proposed scheme is that it is suitable for solutions with sharp edge/jump discontinuities. By slightly modifying the method, the Fibonacci wavelet method can solve the higher-order system of ordinary differential equations and extend to PDEs and other mathematical models with different physical conditions. It is used to obtain the solution of the differential equation in the universal domain by taking the suitable transformation (Figs. 18, 19, 20, 21).

Acknowledgements The authors express their special thanks to Bangalore University for the necessary support.

Author contributions KS proposed the main idea of this paper. KS and MG prepared the manuscript and performed all the steps of the proofs in this research. Both authors contributed equally and significantly to writing this paper. Both authors read and approved the final manuscript.

Funding The authors states that no funding is involved.

Availability of data and materials The data supporting this study's findings are available within the article.

Declarations

Conflict of interest The authors declare that they have no competing interests.

Open Access This article is licensed under a Creative Commons Attribution 4.0 International License, which permits use, sharing, adaptation, distribution and reproduction in any medium or format, as long as you give appropriate credit to the original author(s) and the source, provide a link to the Creative Commons licence, and indicate if changes were made. The images or other third party material in this article are included in the article's Creative Commons licence, unless indicated otherwise in a credit line to the material. If material is not included in the article's Creative Commons licence and your intended use is not permitted by statutory regulation or exceeds the permitted use, you will need to obtain permission directly from the copyright holder. To view a copy of this licence, visit <http://creativecommons.org/licenses/by/4.0/>.

References

1. Park SW, Park DW, Kim TY, Park MY, Oh KJ (2004) Chemical kinetics of the reaction between carbon dioxide and phenyl glycidyl ether using Aliquat 336 as a catalyst. *Catal Today* 98(4):493–498
2. Choe YS, Park SW, Park DW, Oh KJ, Kim SS (2010) The Reaction kinetics of carbon dioxide with phenyl glycidyl ether by TEA–CP–MS41 catalyst. *J Jpn Pet Inst* 53:160–166
3. Subramaniam M, Krishnaperumal I, Lakshmanan R (2012) Theoretical analysis of mass transfer with chemical reaction using the absorption of carbon dioxide into phenyl glycidyl ether solution. *Appl Math* 3:1179–1186
4. Hossein A (2011) An analytical approximation to the solution of chemical kinetics system. *J King Saud Univ Sci* 23(2):167–170
5. Ganji DD, Nourollahi M, Mohseni E (2007) Application of He's methods to nonlinear chemistry problems. *Comput Math Appl* 54(7–8):1122–1132
6. Abbasbandy S, Shirzadi A (2010) Homotopy analysis method for a nonlinear chemistry problem. *Stud Nonlinear Sci* 1(4):127–132
7. Matinfar M, Saeidy M, Gharahsuflu B, Eslami M (2014) Solutions of nonlinear chemistry problems by homotopy analysis. *Comput Math Model* 25(1):103–114
8. Jawary MA, Raham RK (2017) A semi-analytical iterative technique for solving chemistry problems. *J King Saud Univ Sci* 29(3):320–332
9. Kumar R, Kumar S, Singh J, Al-Zhour Z (2020) A comparative study for fractional chemical kinetics and carbon dioxide CO₂ absorbed into phenyl glycidyl ether problems. *AIMS Math* 5(4):3201–3222
10. Robertson H (1966) *Numerical analysis: an introduction* 178–182
11. Jawary MA, Radhi GH (2015) The variational iteration method for calculating carbon dioxide absorbed into phenyl glycidyl ether. *IOSR J Math* 11:99–105
12. Duan JS, Rach R, Wazwaz AM (2015) Steady-state concentrations of carbon dioxide absorbed into phenyl glycidyl ether solutions by the Adomian decomposition method. *J Math Chem* 53:1054–1067
13. Kaya D (2004) A reliable method for the numerical solution of the kinetics problems. *Appl Math Comput* 156(1):261–270
14. Khader MM (2013) On the numerical solutions for chemical kinetics system using Picard–Padé technique. *J King Saud Univ Eng Sci* 25(2):97–103

15. Chowdhury MS, Aznam SM, Mawa S (2021) A novel iterative method for solving chemical kinetics system. *J Low Freq Noise Vib Act Control* 40(4):1731–1743
16. Jawary MA, Rahdi GH, Ravnik J (2020) Boundary-domain integral method and homotopy analysis method for systems of nonlinear boundary value problems in environmental engineering. *Arab J Basic Appl Sci* 27:121–133
17. Singha R, Wazwaz AM (2019) Steady-state concentrations of carbon dioxide absorbed into phenyl glycidyl ether an optimal homotopy analysis method. *Match Commun Math Commun* 81:800–812
18. Shiralashetti SC, Kumbinarasaiah S (2019) Laguerre wavelets collocation method for the numerical solution of the Benjamina–Bona–Mohany equations. *J Taibah Univ Sci* 13(1):9–15
19. Shiralashetti SC, Kumbinarasaiah S (2020) Laguerre wavelets exact Parseval frame-based numerical method for the solution of system of differential equations. *Int J Appl Comput Math* 6(4):1–16
20. Shiralashetti SC, Hoogar BS, Kumbinarasaiah S (2019) Laguerre wavelet-based numerical method for the solution of third-order nonlinear delay differential equations with damping. *Int J Manag Technol Eng* 9:3640–3647
21. Shiralashetti SC, Kumbinarasaiah S (2017) Theoretical study on continuous polynomial wavelet bases through wavelet series collocation method for nonlinear Lane–Emden type equations. *Appl Math Comput* 315:591–602
22. Kumbinarasaiah S, Adel W (2021) Hermite wavelet method for solving nonlinear Rosenau–Hyman equation. *Partial Differ Equ Appl Math* 4:100062
23. Saeed U (2014) Hermite wavelet method for fractional delay differential equations. *J Differ Equ.* <https://doi.org/10.1155/2014/359093>
24. Mundewadi R, Kumbinarasaiah S (2019) Numerical solution of Abel's integral equations using Hermite wavelet. *Appl Math Nonlinear Sci* 4:181–192
25. Rehman M, Khan RA (2011) The Legendre wavelet method for solving fractional differential equations. *Commun Nonlinear Sci Numer Simul* 16:4163–4173
26. Yuttanan B, Razzaghi M (2019) Legendre wavelets approach for numerical solutions of distributed order fractional differential equations. *Appl Math Model* 70:350–364
27. Rahimkhani P, Ordokhani Y, Babolian E (2017) A new operational matrix based on Bernoulli wavelets for solving fractional delay differential equations. *Numer Algorithms* 74:223–245
28. Adel W, Sabir Z (2020) Solving a new design of nonlinear second-order Lane–Emden pantograph delay differential model via Bernoulli collocation method. *Eur Phys J Plus* 35:1–12
29. Ordokhani Y, Rahimkhani P, Babolian E (2017) Application of fractional-order Bernoulli functions for solving fractional Riccati differential equation. *Int J Nonlinear Anal Appl* 8:277–292
30. Xu X, Xu D (2018) Legendre wavelets direct method for the numerical solution of time-fractional order telegraph equations. *Mediterr J Math* <https://doi.org/10.1007/s00009-018-1074-3>
31. Srivastava HM, Shah FA, Irfan M (2020) Generalized wavelet quasi-linearization method for solving population growth model of fractional order. *Math Methods Appl Sci* 43(15):8753–8762
32. Asif M, Haider N, Al-Mdalla QK (2020) A Haar wavelet collocation approach for solving one and two-dimensional second-order linear and nonlinear hyperbolic telegraph equations. *Numer Methods Partial Differ Equ* 36(6):1962–1981
33. Chen CF, Hsiao CH (1997) Haar wavelet method for solving lumped and distributed-parameter systems. *IEE Proc Control Theory Appl* 144:87–94
34. Sadeghian A, Karbassi S, Hushmandasl M, Heydari M (2012) Numerical solution of time-fractional telegraph equation by Chebyshev wavelet method. *Int J Theor Appl Phys* 2(11):163–181
35. Shah FA, Abass R (2019) Solution of fractional oscillator equations using ultraspherical wavelets. *Int J Geom Methods Mod Phys* 16(5):1950075
36. Sabermahani S, Ordokhani Y, Yousefi SA (2020) Fibonacci wavelets and their applications for solving two classes of time-varying delay problems. *Optim Control Appl Methods* 41(2):395–416
37. Sabermahani S, Ordokhani Y (2021) Fibonacci wavelets and Galerkin method to investigate fractional optimal control problems with bibliometric analysis. *J Vib Control* 27(15–16):1778–1792
38. Shiralashetti SC, Lamani L (2020) Fibonacci wavelet based numerical method for the solution of nonlinear Stratonovich Volterra integral equations. *Sci Afr* 10:e00594
39. Firdous AS, Irfan M, Kottakkaran S, Nisar MRT, Mahmoud EE (2021) Fibonacci wavelet method for solving time-fractional telegraph equations with Dirichlet boundary conditions. *Results Phys* 24:104123
40. Irfan M, Firdous AS (2021) Fibonacci wavelet method for solving the time-fractional bioheat transfer model. *Optik* 241:167084
41. Shiralashetti SC, Lamani L (2021) A modern approach for solving nonlinear Volterra integral equations using Fibonacci wavelets. *Electron J Math Anal Appl* 9(2):88–98
42. Srivastava HM, Irfan M, Firdous AS (2021) A Fibonacci wavelet method for solving dual-phase-lag heat transfer model in multi-layer skin tissue during hyperthermia treatment. *Energies* 14(8):2254
43. Kumbinarasaiah S, Manohara G, Hariharan G (2023) Bernoulli wavelets functional matrix technique for a system of nonlinear singular Lane Emden equations. *Math Comput Simul* 204:133–165
44. Sadri K, Hosseini K, Baleanu D, Salahshour S (2022) A high-accuracy Vieta-Fibonacci collocation scheme to solve linear time-fractional telegraph equations. *Waves Random Complex Media* <https://doi.org/10.1080/17455030.2022.2135789>
45. Kumbinarasaiah S, Manohara G (2023) Modified Bernoulli wavelets functional matrix approach for the HIV infection of CD4+ T cells model. *Results Control Optim* 10:100197
46. Richard RG (1963) *Methods of real analysis*. Toronto
47. Robert GB, Donand RS (2014) *Introduction to real analysis*, 3rd edn
48. Srivastava HM, Shah FA, Nayied NA (2022) Fibonacci wavelet method for the solution of the non-linear Hunter–Saxton equation. *Appl Sci* 12(15):7738
49. Sadri K, Hosseini K, Hinçal E, Baleanu D, Salahshour S (2023) A pseudo-operational collocation method for variable-order time-space fractional KdV–Burgers–Kuramoto equation. *Math Methods Appl Sci.* <https://doi.org/10.1002/mma.9015>
50. Hosseini K, Sadri K, Mirzazadeh M, Ahmadian A, Chu YM, Salahshour S (2021) Reliable methods to look for analytical and numerical solutions of a nonlinear differential equation arising in heat transfer with the conformable derivative. *Math Methods Appl Sci.* <https://doi.org/10.1002/mma.7582>
51. Hosseini K, Sadri K, Mirzazadeh M, Salahshour S, Park C, Lee JR (2022) The guava model involving the conformable derivative and its mathematical analysis. *Fractals* 30(10):2240195

Publisher's Note Springer Nature remains neutral with regard to jurisdictional claims in published maps and institutional affiliations.